Wind-induced vibrations monitoring with satellite navigation

Etienne Cheynet, Jasna Bogunović Jakobsen

University of Stavanger, Norway

Jonas Snæbjörnsson

Reykjavik University, Iceland & University of Stavanger, Norway

Contact: etienne.cheynet@uis.no

Abstract

A Global Navigation Satellite System (GNSS) has been deployed on the Lysefjord Bridge in Norway, to measure the static and dynamic displacement of the deck. One objective is to evaluate the systems capability to monitor accurately wind-induced vibrations in high-latitudes and mountainous terrain. GNSS measurements are compared to displacement records obtained from accelerometers located inside the bridge deck. For data of 10 minutes duration, the accelerometers were observed to monitor frequencies below 0.1 Hz with relatively poor accuracy. The GNSS measurements agreed well with the theoretical estimates of the lateral quasi-static bridge response. However, data availability was limited to strong wind conditions only. The completion of the Galileo system in 2020 should expand the applicability and reliability of such systems for structural monitoring purposes in Northern Europe.

Keywords: GNSS; suspension bridge; wind turbulence; buffeting response; accelerometers; structural health monitoring.

1 Introduction

Accelerometers are widely used to measure the dynamic response of civil engineering structures, although their accuracy at low frequencies is not always adequate [1]. For large structures such as future ultra-long span suspension bridges, the resonant part of the displacement is likely to be located close to or below the operating limit of most accelerometers. During the last two decades, Global Navigation Satellite Systems (GNSS) have been promising tools to monitor the static and quasi-static displacements of civil engineering structures [2, 3]. Until now, the focus has mainly been on the development of methodologies and algorithms to assess the accuracy of GNSS measurement technology [4, 5, 6], as well as on testing its capabilities in comparison to accelerometers [7, 8]. Early applications of GPS technology on suspension bridges started at the end of the 90's [9, 10], and expanded since 2000. In particular, applications to modal parameters identification [7, 8, 11], and to wind-induced vibrations analysis of both suspension bridges [12, 13] and tall-buildings [14, 15] have become increasingly popular. Still there are many uncertainties about the complementary role of GNSS and accelerometers in monitoring wind-induced vibrations of long-span suspension bridges. During the summer of 2015, a GNSS base-rover monitoring system was installed at midspan on the deck of the Lysefjord Bridge in Norway. The

data sampling is synchronized to previously installed accelerometers and anemometers [16]. In the present study, GNSS technology is used to record both the quasi-static and dynamic wind induced response of a suspension bridge. The first goal is to evaluate the consistency and accuracy of a GNSS system monitoring of wind-induced vibrations of a suspension bridge in mountainous environment at latitudes above 50°. The second goal is to verify the applicability of the buffeting theory for estimating the quasi-static wind-induced response of a suspension bridge, which was previously done utilizing acceleration data for the frequency range supported by the accelerometers [16].

2 Bridge site and instrumentation

2.1 The Lysefjord Bridge

The Lysefjord Bridge, located at the narrow inlet of a fjord in the South-West part of the Norwegian coast, is used as a study case. Its main span is 446 m, and at midspan the bridge deck is 55 m above the sea level. It is oriented from North-West to South-East in a mountainous environment (Figure 1). It is entrenched between two steep hills with slopes ranging from 30° to 45° and a maximum altitude of 350 m to the North and 600 m to the South. Its East side is exposed to winds that may descent from the mountains nearby or follow the fjord over a longer path. To the West, the bridge is exposed to a more open and levelled area, where the wind may be accelerated in the vicinity of the bridge because of the narrowing effect of the fjord.

Figure 1: South view of the Lysefjord Bridge.

2.2 Accelerometers and anemometers

Between 2013 and 2014, the Lysefjord Bridge has been instrumented with seven sonic anemometers and four pairs of accelerometers placed along the span (Figure 2). Two anemometers are located on hanger 8, denoted H-08, and the others are installed near hangers H-10, H-16, H-18, H-20 and H-24, on the west side of the deck, about six metres above the girder. The distance between each hanger is 12 m, leading to a distance between the anemometers ranging from 24 m to 168 m. The anemometers are 3D WindMaster Pro sonic anemometers, except the one installed on hanger 10, which is a Vaisala weather transmitter WXT520. Wind and acceleration data are synchronized using GPS timing, and continuously transferred to a server via mobile net. The records are filtered and re-sampled at 20 Hz. The displacement data is obtained by transforming the acceleration data into the frequency domain and applying a multiplication scheme, instead of direct integration in the time domain.

2.3 GNSS data

A Real-Time Kinematic-Global Positioning System is used to measure the displacement of the Lysefjord Bridge. Similar systems have previously been used by e.g. Tamura et al. [14] to study wind-induced vibrations of a tall tower. In the present study, a set of Trimble BD930 GNSS receivers are coupled to Trimble AV33 GNSS antennas. These sensors can handle data sampling at a frequency of 20 Hz, with an accuracy of $\pm 8\,mm + 1ppm$ for the horizontal displacement and $\pm 15\,mm + 1ppm$ for the vertical displacements. The base-rover combination may increase measurement accuracy, as it is the relative displacement between a “fixed” base station and a “moving” rover station that is monitored.

The GNSS base-rover monitoring system measures the displacement at mid-span in the East, North and vertical directions. Therefore, the lateral and vertical bridge displacement can be directly obtained using Eq. 1, where θ is the bridge orientation with respect to North, equal to 40.5°.

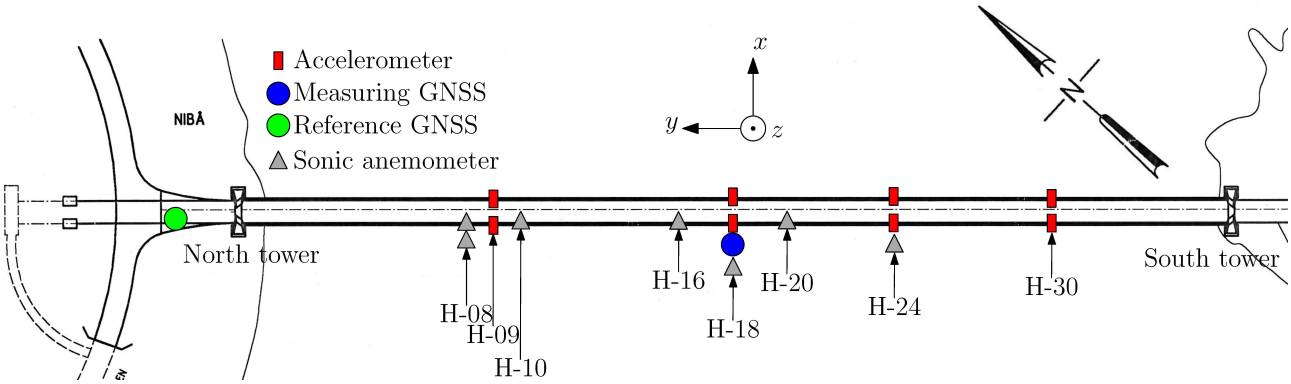

Figure 2: Sensors installed along the bridge deck. Anemometers are represented by grey triangles; GNSS sensors are visible as one blue and green dot; accelerometers are depicted as red rectangles.

$$\begin{bmatrix} D_x \\ D_y \\ D_z \end{bmatrix} = \begin{bmatrix} \cos(\theta) & \sin(\theta) & 0 \\ -\sin(\theta) & \cos(\theta) & 0 \\ 0 & 0 & 1 \end{bmatrix} \begin{bmatrix} D_E \\ D_N \\ D_H \end{bmatrix} \quad (1)$$

3 Static and dynamic analysis

Wind data from N-NE that is recorded on 07/10/2015 is used for both the static and the dynamic analysis. The analysis relies on calculations in the modal base, assuming homogeneous and stationary flow. Modal coupling is neglected, and only the vertical and lateral displacements are investigated. The first four lateral and vertical modes are taken into account, and are provided by a finite element model [17]. To improve the accuracy of the computed response, slight discrepancies between the computed and measured eigen-frequencies were corrected.

In the present study, the static displacement is computed for the lateral direction only, and is obtained using a multimodal approach, as seen in Eq. (2):

$$\boldsymbol{D_{ox}} = \boldsymbol{\Phi}^{\intercal} (\boldsymbol{K^{-1}}) \boldsymbol{F_D} \quad (2)$$

where $\boldsymbol{\Phi}$ is a N_m by N_y matrix of mode shapes, where N_m is the number of modes and N_y is the number of integrations points along the suspension bridge modelled as a line segment. The matrix of modal stiffness $\boldsymbol{K}$ is a N_m by N_m matrix, and $\boldsymbol{F_D}$ is a N_m by 1 vector of the static modal load, calculated using data provided in [16].

The dynamic response to wind turbulence is undertaken in the frequency domain, based on the buffeting theory [18], and the quasi-steady theory [19], using the same numerical model as in [16]. The single point wind spectrum is obtained by averaging the measured wind spectra on hangers 16, 18 and 20. The co-coherence is approximated by a simple exponential decay function as used by Davenport [20]. The spectral densities are computed using Welch's overlapped segment averaging estimator, based on 10 minutes long data series divided into blocks of 300 seconds, using shorter blocks of 60 seconds to reduce the aleatory variability and the bias error in the estimate [21].

4 Results and discussions

4.1 Static analysis

Nakamura [12] observed a good agreement between the static lateral displacement computed with a finite element model of a suspension bridge and the one measured from a wind tunnel model using GPS technology. For a full-scale bridge, he noted a considerable scatter, which might have been due to multipath effects, signal distortion due to ionosphere and troposphere delays, cycle slips, high noise to signal ratio, non-stationary wind conditions, or temperature variations.

For data recorded on 07/10/2015, we observed that high number of samples were affected by cycle slips [22]. Cycle slips are discontinuities in the recorded signal due to temporary signal loss, which were here probably due to bad satellite coverage, caused by high latitude location, mountainous terrain surrounding the bridge and possibly some

shadowing effects from the bridge tower. Because the measurement of the static displacement requires stationary wind conditions, the reverse arrangement test [23] was applied to select only stationary displacement records. This led to a significant reduction of the scatter of measured static displacement, because both cycle slips and non-stationary bridge records were eliminated. The measured static displacements are divided by the deck width, denoted B, and expressed as a function of the mean wind component normal to the deck, V_x in Figure 3. A satisfying agreement was then observed, between the measured and computed lateral static displacement in Figure 3.

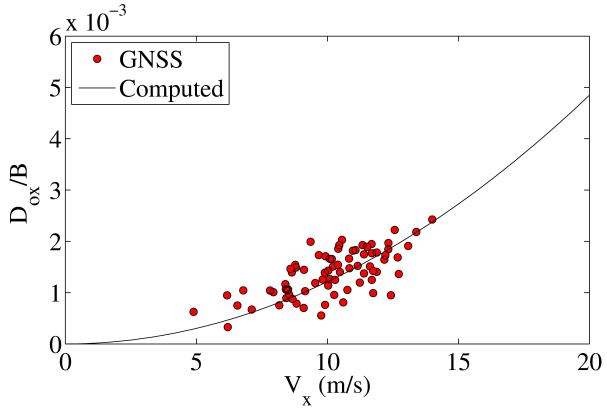

Figure 3: Lateral static displacement measured at midspan, on 07/10/2015, based on 10-minutes averaged displacement data from the GNSS.

4.2 Dynamic analysis

4.2.1 Single sample

The time histories and the power spectral density (PSD) of the bridge displacement response recorded on 07/10/2015 between 05:20 and 05:30 is used as a study case. A stationary flow from the N-NE was monitored, with a mean wind velocity at mid span of 11.7 m/s, and turbulence intensities I_u = 31 % and I_w = 12 %. The along-wind integral length scales L_u and L_w were equal to 110 m and 37 m respectively. In the present study, the measured co-coherence was fairly well approximated by the single exponential decay. The decays coefficients C_u^y and C_w^y were found to be equal to 8.4 and 5.7 respectively. As highlighted by e.g. [24, 1], accelerometers usually show limited capabilities in monitoring vibrations below a given frequency threshold, which is here observed to range from 0.06 to 0.1 Hz.

A direct comparison between the PSD of the accelerometers and the GNSS system in Figure 4 shows that more measurement noise is present in the GNSS record than in the accelerometer data for frequencies above 0.5 Hz. Both sensors capture properly the first eigen-frequency, which is located around 0.30 Hz for the vertical direction and 0.13 Hz for the lateral one. Below frequencies corresponding to the first resonant peak, the accelerometer indicates somewhat larger displacement response although The GNSS and accelerometers data agree well down to 0.1 Hz. Below 0.1 Hz the difference between the two measurement techniques becomes non-negligible, and illustrates the limitations of accelerometers in monitoring displacement responses at low frequencies.

The PSD of the computed vertical displacement is lower than the one measured by the GNSS at low frequencies (Figure 4). For the lateral displacement, the computed and measured quasi static response show however a good agreement. The limiting resolution of the vertical displacement results in a more or less constant measurement noise over the whole frequency range. However, this noise does not explain the discrepancy between the quasi-static part of the measured and computed PSD for the vertical response. The influence of the torsional angle of the bridge deck, which cannot be removed if the displacement is monitored at one point only, may be responsible for this discrepancy. The coherence model we used in the present study may also underestimate wind coherence at low frequencies. The application of the 3-parameter exponential decay model used in [16] did not improve the estimated vertical PSD. Better estimation of wind coherence at low frequencies requires analysis using wind data of duration larger than 10 minutes.

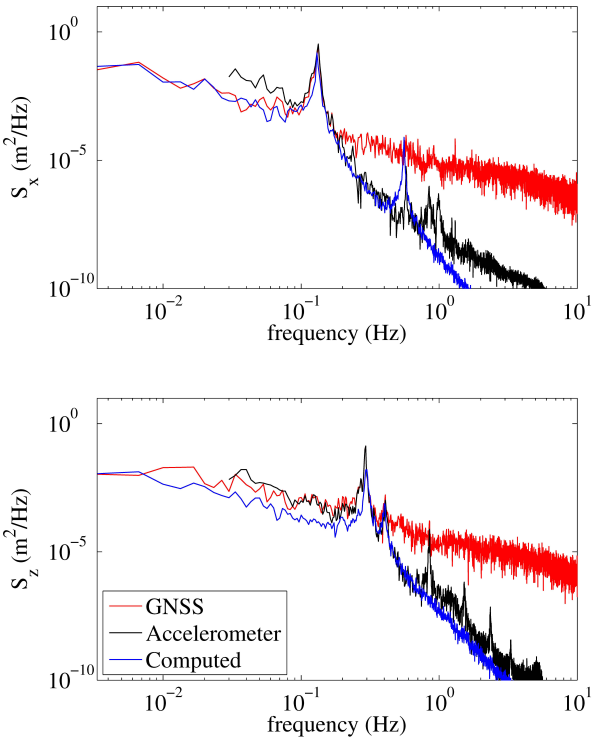

Figure 4: PSD of the lateral (top) and vertical (bottom) bridge displacement responses recorded near H-18, on 07/10/2015 between 05:20 and 05:30.

In Figure 5, the direct comparison in the time domain between the GNSS and the accelerometer data shows a good agreement for both the lateral and the vertical direction. A slightly higher noise is visible for the vertical direction, which is expected given the technical specifications of the GNSS. A lower measurement accuracy is generally observed for the vertical displacements compared to the horizontal ones [3]. Sub-centimetre down to a millimetre level accuracy can be achieved by modern GNSS technology. By using a motion simulation table, Chan et al. [4] measured horizontal and vertical displacements with an accuracy up to 5 mm and 10 mm respectively. By simulating harmonic displacement with a rotating GPS antenna, Nickitopoulou et al. [6] observed that an accuracy of 15 mm for the horizontal displacements and 35 mm for the vertical ones was permitted at 1.5 % outlier level. More recently, a sub-millimetre accuracy was achieved by Yu et al [8] by using a higher number of GNSS antenna. In the present study, the standard deviation for the lateral and vertical dynamic displacement are 5 mm and 4 mm respectively. This indicates that the vertical displacements recorded are close to the operative limits of the GNSS used.

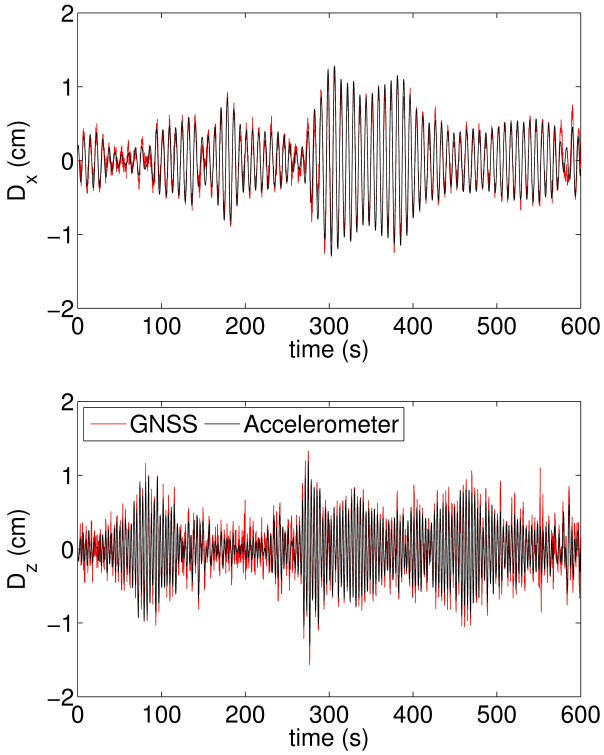

Figure 5: Vertical (top) and lateral (bottom) resonant wind-induced bridge response near H-18, on 07/10/2015 between 05:20 and 05:30.

4.2.2 Multiple samples

For a full day of records, the dynamic displacement at mid-span was obtained by applying a band-pass filter with an upper and lower cut-off frequency of 1 Hz and 0.1 Hz to the total measured deck displacement. The lower boundary is chosen so that the accelerometer data provides a reliable comparison. The upper boundary is chosen so that the first four eigen-modes in each direction are taken into account, providing a good overview of the resonant response. In addition, this procedure allows removing possible torsional resonant responses at around 1.2 Hz, which might complicate the interpretation of the displacement data.

Figure 6 compares the RMS of the dynamic displacements measured by the GNSS with those obtained with the accelerometer on H-18. We observed a good agreement for the lateral displacement, but for the vertical one, the GNSS instruments provide systematically higher values of

resonant displacement response than the accelerometer data, which is consistent with Figure 4 and Figure 5. The presence of measurement noise associated by the combination of vertical and torsional displacement may be responsible for the overestimation of the vertical resonant response measured by the GNSS. A higher noise is generally observed in the GNSS data. At low wind velocities, the data quality may be too poor to accurately monitor the Lysefjord Bridge displacement. For larger suspension bridges, the influence of measurement noise should be mitigated because larger displacements of the deck are expected. In addition, estimation of the GNSS measurement noise during a calibration procedure [11] should reduce the systematic error between the accelerometers and the GNSS for the vertical displacement.

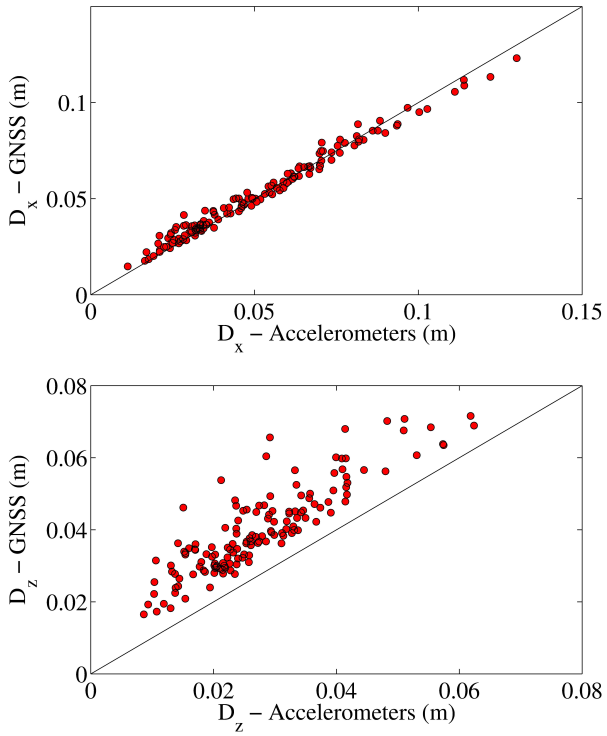

Figure 6: Standard deviation of the dynamic displacements measured by the GNSS sensor compared to the accelerometers data at mid-span, in the range [0.1-1.0 Hz]. The continuous line refers to the ideal case of a perfect correlation between the accelerometers and GNSS measurements.

4.3 Challenges and prospects

Some current large suspensions bridges in Norway have already natural frequencies close or below the operative limit of most accelerometers. For example, the first symmetrical lateral eigen-frequency of the Hardanger Bridge is 0.05 Hz, and its first asymmetric vertical eigen-frequency is 0.11 Hz. For future ultra-long span suspension bridges, even lower eigen-frequencies are expected as highlighted by [25], meaning that GNSS sensors may play a central role in structural health monitoring. The static and dynamic displacements are likely to be much larger than those recorded at Lysefjord Bridge, which should increase the amount of high-quality data obtained with GNSS systems. However, the latitude of Norway is well above 50°, which is the limit beyond which the availability of satellite constellations start reducing [6, 26]. Consequently, the quality of results is expected to be poorer than for mid-latitudes. In the present study, the amplitude of wind-induced vibrations for wind from S-SW were for example often too low to be captured in details by the GNSS rover. Fortunately, the deployment of the Galileo system in 2020 [27] should improve the accuracy of GNSS positioning in Northern Europe.

5 Conclusions

Wind-induced vibrations of a suspension bridge have been investigated in details using GNSS base-rover devices. Comparisons with three-axial accelerometers have shown that GNSS observations play a complementary role that may become predominant for ultra-long span suspensions bridges. Because of the relative short span of the Lysefjord Bridge, the dynamic displacement for the vertical DOF was close to the operative limit of the GNSS, for the wind velocities studied, and a non-negligible measurement noise was obtained. The GNSS and accelerometers showed however a good agreement for the dynamic and static lateral displacements. A good signal to noise ratio for the vertical displacement was obtained under strong wind conditions only, which limited the quantity of available data. The high latitude of the Lysefjord Bridge may also at least partly be responsible for lack of data quality at low excitation levels. The deployment of the

Galileo system should improve the accuracy of GNSS measurements in Europe and consequently strengthen the development of GNSS monitoring systems as a complementary tool for structural health monitoring of large civil engineering structures.

6 Acknowledgements

The authors would like to gratefully acknowledge the support of the Norwegian Public Roads Administration to the measurement campaign, as well as to the installation and maintenance of the monitoring system.

7 References

[1] Xu, Y.L. and Xia, Y., Structural Health Monitoring of Long-Span Suspension Bridges, CRC Press, 2011.

[2] Lovse, J. W., Teskey, W. F., Lachapelle, G., & Cannon, M. E. , "Dynamic deformation monitoring of tall structure using GPS technology," *Journal of surveying engineering,* vol. 121, no. 1, pp. 35-40, 1995.

[3] Im, S. B., Hurlebaus, S., & Kang, Y. J., "Summary Review of GPS Technology for Structural Health Monitoring," *Journal of Structural Engineering,* vol. 139, pp. 1653-1664, 2013.

[4] Chan, W. S., Xu, Y. L., Ding, X. L., Xiong, Y. L., and Dai, W. J., "Assessment of Dynamic Measurement Accuracy of GPS in Three Directions," *Journal of Surveying Engineering,* vol. 132, no. 3, pp. 108-117, 2006.

[5] Chan, W. S., Xu, Y. L., Ding, X. L., & Dai, W. J., "An integrated GPS–accelerometer data processing technique for structural deformation monitoring," *Journal of Geodesy,* vol. 80, pp. 705-719, 2006.

[6] Nickitopoulou, A., Protopsalti, K., and Stiros, S., "Monitoring dynamic and quasi-static deformations of large flexible engineering structures with GPS: accuracy, limitations and promises," *Engineering Structures,* vol. 28, no. 10, pp. 1471-1482, 2006.

[7] Meng, X., Dodson, A. H., & Roberts, G. W. , "Detecting bridge dynamics with GPS and triaxial accelerometers," *Engineering structures,* vol. 29, pp. 3178-3184, 2007.

[8] Yu, J., Meng, X., Shao, X., Yan, B., and Yang, L., "Identification of dynamic displacements and modal frequencies of a medium-span suspension bridge using multimode GNSS processing," *Engineering Structures,* vol. 81, pp. 432-443, 2014.

[9] Ashkenazi, V., & Roberts, G. W., "Experimental monitoring of the Humber Bridge using GPS," in *Proceedings of the Institution of Civil Engineers-Civil Engineering*, 1997.

[10] Fujino, Y., Murata, M., Okano, S., & Takeguchi, M., "Monitoring system of the Akashi Kaikyo Bridge and displacement measurement using GPS," in *SPIE's 5th Annual International Symposium on Nondestructive Evaluation and Health Monitoring of Aging Infrastructure*, 2000.

[11] Roberts, G., Meng, X., and Dodson, A., "Integrating a global positioning system and accelerometers to monitor the deflection of bridges," *Journal of Surveying Engineering,* vol. 130, no. 2, pp. 65-72, 2004.

[12] Nakamura, S. I., "GPS Measurement of Wind-Induced Suspension Bridge Girder Displacements," *Journal of Structural Engineering,* 2000.

[13] Xu, Y. L., & Chan, W. S., "Wind and structural monitoring of long span cable-supported bridges with GPS," in *The Seventh Asia-Pacific Conference on Wind Engineering: APCWE-VII*, Taipei, 2009.

[14] Tamura, Y., Matsui, M., Pagnini, L. C., Ishibashi, R., and Yoshida, A., "Measurement of wind-induced response of buildings using RTK-GPS," *Journal of Wind Engineering and Industrial Aerodynamics,* vol. 90, no. 12, pp. 1783-1793, 2002.

[15] Kijewski-Correa, T., Kareem, A., & Kochly, M. , "Experimental verification and full-scale deployment of global positioning systems to monitor the dynamic response of tall buildings," *Journal of Structural Engineering,* vol. 132, no. 8, pp. 1241-1253, 2006.

[16] Cheynet, E., Jakobsen, J. B., and þór Snæbjörnsson, "Buffeting response of a bridge at the inlet of a fjord," in *ICWE14: 14th International Conference on Wind Engineering*, Porto Alegre, 2015.

[17] AAS-Jakbosen, "Beregninger av egenfrekvenser for lysefjordbrua," for the Norwegian Public Road Adminitration, 1999.

[18] R. H. Scanlan, "The action of flexible bridges under wind, II: Buffeting theory," *Journal of Sound and vibration,* vol. 60, no. 2, pp. 201-211, 1978.

[19] J. D. Holmes, Wind Loading of Structures, CRC Press, 2007.

[20] A. G. Davenport, "The spectrum of horizontal gustiness near the ground in high winds," *Quarterly Journal of the Royal Meteorological Society,* vol. 87, no. 372, pp. 194-211, 1961.

[21] Kristensen L., Kirkegaard P., Sampling problems with spectral coherence, Risø National Laboratory, 1986.

[22] Hofmann-Wellenhof, B., Lichtenegger, H., & Wasle, E. , GNSS - Global Navigation Satellite Systems: GPS, GLONASS, Galileo, and more, Springer Vienna, 2007.

[23] Bendat, J. S., & Piersol, A. G. , Random data: analysis and measurement procedures, John Wiley & Sons, 2011.

[24] Moschas, F., & Stiros, S. , "Dynamic multipath in structural bridge monitoring: an experimental approach," *GPS Solutions,* vol. 18, pp. 209-218, 2014.

[25] Fujino, Y., & Siringoringo, D., "Vibration mechanisms and controls of long-span bridges: A Review," *Structural Engineering International,* vol. 23, no. 3, pp. 248-268, 2013.

[26] Breuer, P., Chmielewski, T., Górski, P., & Konopka, E. , "Application of GPS technology to measurements of displacements of high-rise structures due to weak winds," *Journal of Wind Engineering and Industrial Aerodynamics,* vol. 90, no. 3, pp. 223-230, 2002.

[27] ESA, "Galileo fact sheet," 2012. [Online]. Available: http://download.esa.int/docs/Galileo_IOV_Launch/Galileo_factsheet_2012.pdf. [Accessed 15 02 2013].